

Fractionated single-particle states of ^{31}Si at $E_x = 5.3\text{--}9.4$ MeV[†]

G. W. Hoffmann, J. McIntyre, and W. R. Coker

Center for Nuclear Studies, University of Texas, Austin, Texas 78712

(Received 18 July 1974)

A total of 40 states of ^{31}Si in the region of excitation from about 5 to 9 MeV have been studied using the reaction $^{30}\text{Si}(d, p)$ at 10 MeV incident deuteron energy, and a biased quadrupole spectrometer. Fractionated single-particle states are identified via their forward-angle cross sections, using distorted-wave Born-approximation predictions with bound and resonance state form factors for the residual ^{31}Si system. Results are contrasted with what is known of the lower lying states, from large-basis shell-model calculations and earlier (d, p) experiments.

[NUCLEAR REACTIONS $^{30}\text{Si}(d, p)$, $E_d = 10$ MeV, measured $\sigma(\theta)$. ^{31}Si deduced levels, l , j , π , spectroscopic factors. Enriched target.]

I. INTRODUCTION

There have been a large number of rather thorough studies of the low-lying states of almost all the nuclei close to the line of β stability, in which heavy reliance has been placed on direct reaction spectroscopy. However, relatively few studies have continued for more than a few MeV in excitation in the residual nucleus, since above a few MeV the single-particle strength of even the most strongly populated states drops below 0.1 and the level spacing becomes quite small; there are also a number of experimental problems, mainly due to high backgrounds.

However, recent work on states in $^{37, 39, 41}\text{Ar}$ at excitation energies of 5 to 8 MeV, excited via $^{36, 38}\text{Ar}(d, p)^1$ and $^{40}\text{Ar}(d, p)^2$ has shown that fairly conventional direct reaction spectroscopy may be carried out at such excitations in this mass region. The angular distributions of the observed states, from 10° to 150° , showed clear stripping patterns consistent with those predicted by the conventional distorted-wave Born-approximation (DWBA) description of direct nuclear reactions.¹ The particular orbital angular momentum transfer involved in the (d, p) reaction can easily be identified from the slope of the experimental angular distribution in the angular range from 10° to 90° . This distinctiveness of slope is illustrated in Fig. 1 for $^{30}\text{Si}(d, p)^{31}\text{Si}$ to a state at 6.81 MeV, assuming 10 MeV incident deuteron energy. Since backgrounds are quite high in the region of nuclear excitation near the neutron separation energy, despite the use of charge and mass separation techniques, it is still something of a challenge to obtain data which has good enough statistical quality to decide, for instance, between $l=2$ and $l=3$.

In the present work, we have studied states in ^{31}Si between 5.8 and 9.4 MeV in excitation, via the

$^{30}\text{Si}(d, p)$ reaction at 10 MeV incident deuteron energy. At this particular energy, the difference in slope between $l=1, 2$, and 3 transfers is large, facilitating the spectroscopic analysis. A total of 40 states was observed in the region of excitation covered. Reasonably complete angular distributions, covering about 10° to 70° center-of-mass angle, could be obtained for 26 of these states, with partial angular distributions for about five more. In what follows, we present these data, as well as the results of a DWBA analysis making use of Gamow-state form factors to describe the unbound residual states.¹ We further view our work in the perspective of earlier studies of lower-lying states of ^{31}Si ^{3,4} and of predictions of the shell model. Finally, we summarize our present understanding of the distribution of single-particle neutron strength, particularly for $d_{3/2}$ and $f_{7/2}$ neutron states, in the region of 6 to 9 MeV excitation in ^{31}Si .

II. EXPERIMENTAL PROCEDURE

A 10-MeV deuteron beam from the University of Texas EN tandem accelerator was used to bombard a self-supporting SiO target of ^{30}Si isotopic enrichment $> 99\%$. Target thickness was approximately $150 \mu\text{g}/\text{cm}^2$, and the beam current used throughout the experiment was 350–400 nA. The biased quadrupole spectrometer⁵ recently developed at the Center for Nuclear Studies was used to achieve perfect particle identification while enabling the use of a single high-resolution charged particle detector. Briefly, protons within a given energy range $E \pm dE$, after passing through an offset slit, are focused through a second slit in front of the detector, while deuterons of energies within this same range $E \pm dE$ are stopped by the second slit. For a given quadrupole magnetic field setting, the range $\pm dE/E$ of protons focused

through the second slit onto the detector is typically $\pm 10\%$ for the slit geometry used in this experiment.

The solid state detector was a lithium-drifted silicon detector of thickness 2 mm, cooled to dry ice temperature by means of a cold finger. Since the particle detector is approximately 2 m from the target, noise in the detector resulting from neutron, γ , and electron radiation is greatly reduced. Yet the effective solid angle for those protons focused by the spectrometer is 1.0 msr. Since the elastically scattered deuterons had energies near 10 MeV, they could not reach the detector unless the quadrupole spectrometer was adjusted to focus 20-MeV protons; hence, small (d,p) cross sections could be measured routinely down to 5° c.m. scattering angle.

A Tennelec TC135 preamplifier followed by an ORTEC 452 spectroscopy amplifier provided linear energy signals which were subsequently stretched by a Tennelec TC621 stretcher multiplexer and

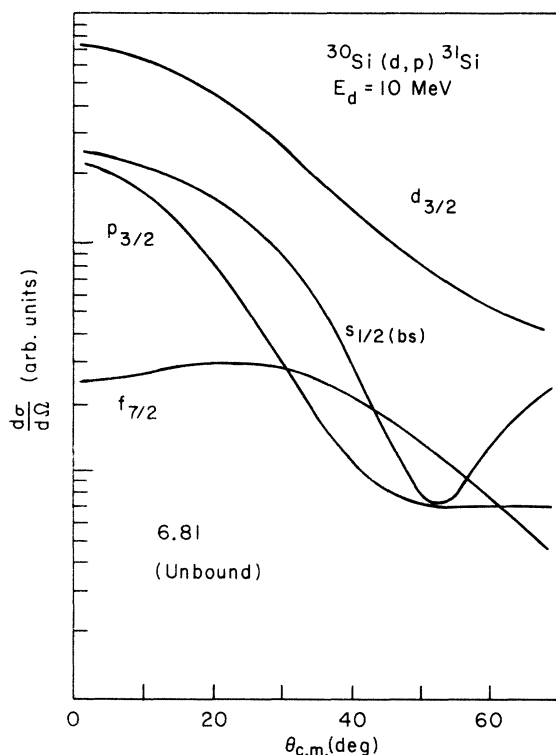


FIG. 1. Typical DWBA predictions for angular distributions of the reaction $^{30}\text{Si}(d,p)^{31}\text{Si}$ at 10 MeV incident deuteron energy, to a state at 6.81 MeV in excitation. The form factors used for the calculations are in each case complex energy eigenstates corresponding to a resonance at 0.22 MeV neutron energy, except in the case of the $s_{1/2}$ transition where a state bound by 0.1 MeV was assumed. The difference in slope between $p_{3/2}$ and $d_{3/2}$ is actually greater than depicted here at higher excitations.

digitized by a Tennelec TC501 analog-to-digital convertor for input to a PDP-7 computer where 4096-channel energy spectra were accumulated. The "BUSY OUT" signal of the Tennelec stretcher was used to inhibit the BNC 1000 C current integrator, connected to a small Faraday cup inside the scattering chamber, for automatic dead time correction whenever the stretcher was busy.

Angular distributions were taken for three magnetic field settings of the quadrupole spectrometer. These were chosen to center the proton window at laboratory energies of 7.4, 6.2, and 5.0 MeV, corresponding to excitation energies in ^{31}Si of 7.0, 8.2, and 9.4 MeV, respectively. In this way states of excitation $E_x = 6$ to 10 MeV could be examined.

Over-all experimental resolution was 14 keV, full width at half-maximum. The principal source of experimental error was due to uncertainty in background subtraction, not to poor statistical accuracy. The background presumably arises largely from (d,p) reactions on oxygen, carbon nitrogen, and lighter contaminants, and possible (d,α) processes (the quadrupole spectrometer cannot distinguish between protons and ^4He nuclei of the same energy).

States in ^{31}Si populated via $^{30}\text{Si}(d,p)$ were identified by kinematic tracking. Calibration and excitation energies were verified by identifying 12 of the lowest lying states seen in this experiment with those previously observed.⁶

III. GENERAL DISCUSSION OF THE DATA

Of the 40 states in ^{31}Si which we observed, 26 had extractable angular distributions. The excitation energies of all the states observed in this experiment are given in Table I, together with spectroscopic information to be discussed in Sec. IV. The excitation energies of 12 of the states in our experiment were also measured by Hinds and Middleton,⁶ and our energies agree with theirs to within experimental error (± 5 keV). The majority of the states listed in Table I have not been observed previously.

The angular distributions we obtained are shown in Figs. 3 through 5. To supplement our results, we have included in our analysis data obtained by Betigeri *et al.*⁴ Six angular distributions of states in the excitation range from 5.2 to 6.2 MeV are shown in Fig. 2, together with results of our DWBA analyses, to be discussed later. The data of Betigeri *et al.* are consistent with our own data for those states observed in common, as illustrated for the 6.24-MeV state in Fig. 3, where our data are shown as circles and the data of Betigeri *et al.* are shown as triangles. There is excellent

TABLE I. States of ^{31}Si , between 5.27 and 9.38 MeV in excitation, observed in the present experiment. Where angular distributions could be obtained, l_j values and spectroscopic factors C^2S are assigned. Where angular distributions are incomplete, only a rough peak cross section is usually tabulated. A value in parentheses is uncertain.

| E_x (MeV) | l | l_j^a | C^2S | Γ_n^{sp} (keV) | σ_{max} (mb/sr) |
|-------------------|--------|---------------------|----------|---------------------------------|----------------------------------|
| 5.27 | 0 | $s_{\frac{1}{2}}$ | 0.038 | ... | ... |
| 5.43 | (2) | $(d_{\frac{3}{2}})$ | (0.067) | ... | ... |
| 5.82 ^b | ... | ... | ... | ... | 0.2 ± 0.1 (15°) |
| 5.87 ^b | 1 | $p_{\frac{3}{2}}$ | 0.038 | ... | ... |
| 5.95 ^b | (2) | $(d_{\frac{3}{2}})$ | (0.023) | ... | ... |
| 6.07 ^b | 2 | $d_{\frac{3}{2}}$ | 0.020 | ... | ... |
| 6.10 ^b | 3 | $f_{\frac{7}{2}}$ | 0.036 | ... | ... |
| 6.24 ^b | 2 | $d_{\frac{3}{2}}$ | 0.067 | ... | ... |
| 6.34 ^b | ... | ... | ... | ... | 0.25 ± 0.1 (15°) |
| 6.39 | ... | ... | ... | ... | 0.5 ± 0.1 (25°) |
| 6.45 ^b | ... | ... | ... | ... | 0.8 ± 0.2 (15°) |
| 6.58 ^b | ... | ... | ... | ... | 0.13 ± 0.05 (40°) |
| 6.65 ^b | ... | ... | ... | ... | 0.10 ± 0.05 (40°) |
| 6.78 | ... | ... | ... | ... | 0.14 ± 0.05 (40°) |
| 6.81 ^b | (2) | $(d_{\frac{3}{2}})$ | (0.050) | 4.6 | ... |
| 6.87 ^b | ... | ... | ... | ... | 0.20 ± 0.05 (40°) |
| 6.90 | 2 | $d_{\frac{3}{2}}$ | 0.022 | 12.0 | ... |
| 6.94 | 2 | $d_{\frac{3}{2}}$ | 0.011 | 14.0 | ... |
| 7.29 | ... | ... | ... | ... | 0.20 ± 0.10 (15°) |
| 7.42 | 2 | $d_{\frac{3}{2}}$ | 0.024 | 106.0 | ... |
| 7.63 | (2, 3) | ... | ... | ... | 0.08 ± 0.04 (30°) |
| 7.88 | (3) | $(f_{\frac{7}{2}})$ | (0.0025) | (24.8) | ... |
| 7.99 | 3 | $f_{\frac{7}{2}}$ | 0.0076 | 32.3 | ... |
| 8.01 | | | | | |
| 8.04 | | | | | |
| 8.09 | | | | | |
| 8.14 | 3 | $f_{\frac{7}{2}}$ | 0.007 | 43.6 | ... |
| 8.22 | ... | ... | ... | ... | ... |
| 8.24 | (3) | $(f_{\frac{7}{2}})$ | (0.0015) | (51.4) | 0.05 ± 0.04 (20°) |
| 8.36 | 3 | $f_{\frac{7}{2}}$ | 0.015 | 64.8 | ... |
| 8.57 | 2 | $d_{\frac{3}{2}}$ | 0.0018 | 745.0 | ... |
| 8.62 | 2 | $d_{\frac{3}{2}}$ | 0.0055 | 792.0 | ... |
| 8.71 | (3) | $(f_{\frac{7}{2}})$ | (0.002) | (108.0) | ... |
| 8.78 | (2) | $(d_{\frac{3}{2}})$ | (0.001) | (937.0) | ... |
| 8.83 ^c | (1) | $(p_{\frac{3}{2}})$ | ... | ... | 0.10 ± 0.05 (10°) |

TABLE I. (Continued)

| E_x (MeV) | l | l_j^a | C^2S | Γ_n^{sp} (keV) | σ_{max} (mb/sr) |
|-------------------|-----|---------------|---------|--------------------------|---------------------------|
| 8.85 | ... | ... | ... | ... | $0.05 \pm 0.04(10^\circ)$ |
| 8.92 ^c | (1) | $(p_{3/2}^2)$ | ... | ... | $0.05 \pm 0.01(10^\circ)$ |
| 8.97 ^c | (1) | $(p_{3/2}^2)$ | ... | ... | $1.2 \pm 0.3(10^\circ)$ |
| 9.23 | (2) | $(d_{3/2}^2)$ | (0.001) | (1474.0) | ... |
| 9.38 | ... | ... | ... | ... | $0.05 \pm 0.02(20^\circ)$ |

^aAs assumed in the DWBA analysis.

^bA state of this excitation was also reported in Ref. 6.

^cSee text.

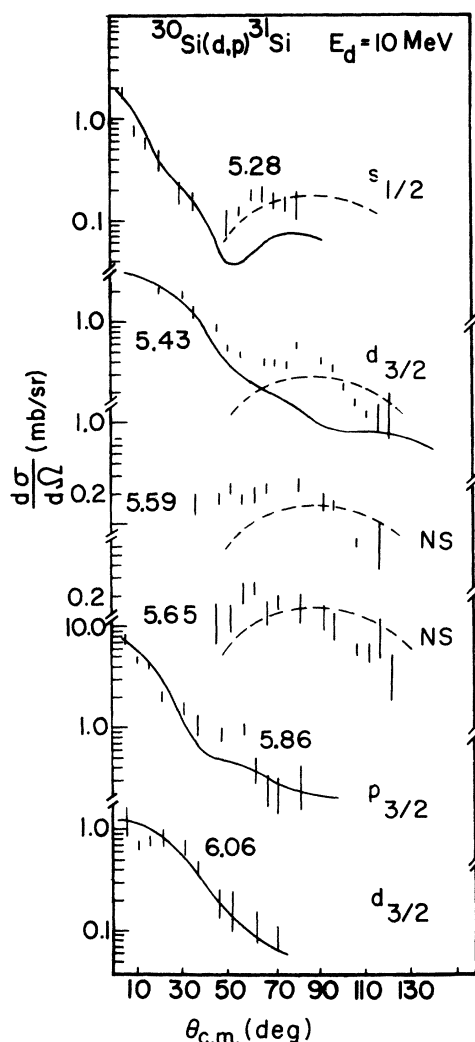


FIG. 2. Experimental angular distributions and DWBA calculations for states of ^{31}Si ranging from 5.28 to 6.06 MeV in excitation. The solid curves are DWBA predictions, obtained as explained in the text. The dashed curves are "fits" by eye to apparent compound nuclear contributions, and are labeled NS for nonstripping. Extracted spectroscopic factors are summarized in Table I. Data are from Ref. 4.

agreement, in both shape and magnitude. The systematic errors depicted by bars in Figs. 3 through 5 are typically 20% and are due principally to uncertainties in background subtraction procedures. The anticipated error in the absolute cross section is also about 20%, in each case.

The incident energy of 10 MeV was chosen for two reasons: first, to facilitate comparison with earlier work on ^{31}Si ^{3,4}; and, second, to obtain angular momentum matching for $l=1$. As a result of this matching, the angular distributions are

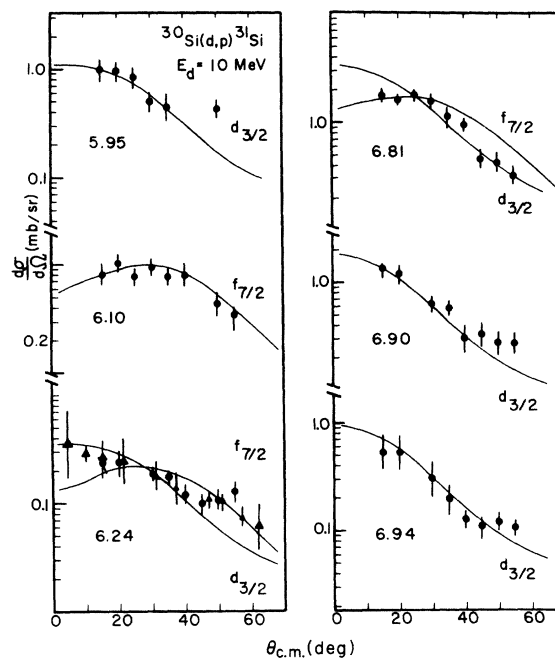


FIG. 3. Experimental angular distributions and results of DWBA calculations for states of ^{31}Si ranging from 5.95 to 6.94 MeV in excitation. The solid curves are DWBA predictions, as in Fig. 2. Extracted spectroscopic factors are summarized in Table I. The data points shown as triangles for the 6.24-MeV state are from Ref. 4.

quite distinctive of the l transfer, even for excitations of 8 to 9 MeV. Over the entire range of excitation covered, in the angular range from 0° to 90° in the center-of-mass, the slopes of $l=1, 2,$ and 3 transitions are progressively less and less abrupt, as the fits shown in Figs. 2–5 illustrate strikingly. Thus it is possible to determine the orbital angular momentum of the ^{31}Si levels with surprisingly little uncertainty, despite the high background and resulting scatter of the angular distribution data. At higher incident energies, this good matching is lost; for example, at 16-MeV incident energy, it becomes almost impossible to distinguish between $l=1$ and 3 for states at excitations of 8 to 9 MeV, except at extreme forward angles (see Ref. 7).

Most of the angular distributions observed had the slopes expected from a (d,p) stripping mechanism. Two exceptions are the states at 5.59 and 5.65 MeV, shown in Fig. 2, both with peak cross sections of 0.2 mb/sr at 90° , and rough symmetry about 90° . The dashed curves in Fig.

2 are fits by eye to the trend of these nondirect cross sections; they are labelled NS, for “non-stripping.” Similar contributions, of the same magnitude, can be made out in the angular distributions for the 5.27- and 5.43-MeV states, but they do not affect the stripping patterns. At higher excitations, the only states which have extractable cross sections are those with distinct forward angle peaks, so that compound contributions are not a problem.

IV. DWBA ANALYSIS AND DISCUSSION OF RESULTS

Of the 26 states for which we have calculated angular distributions, 19 are unbound. These states were described using a technique developed by Coker.^{1,8,9} Complex energy eigenstates were computed using the program GAMOV-3, as described in Ref. 1, and these eigenstates functions were used as form factors in distorted wave Born approximation (DWBA) calculations with the program VENUS.¹⁰ For the bound states, form

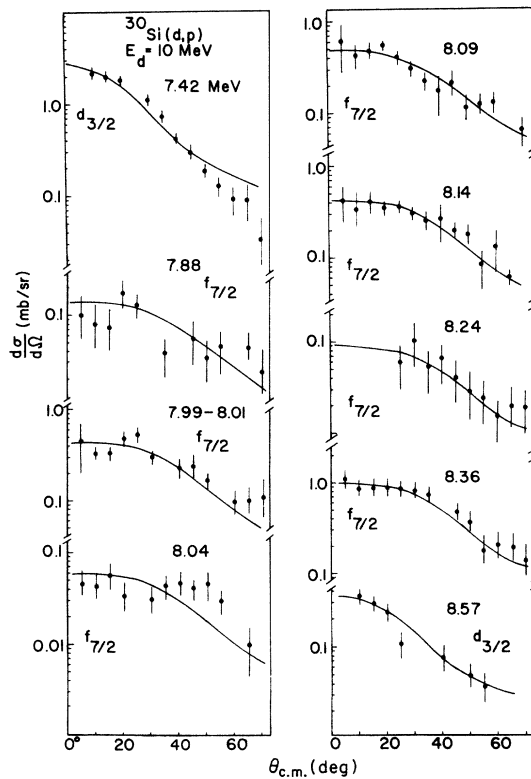


FIG. 4. Experimental angular distributions and results of DWBA calculations for states of ^{31}Si ranging from 7.42 to 8.57 MeV in excitation. The solid curves are DWBA predictions, and extracted spectroscopic factors are summarized in Table I.

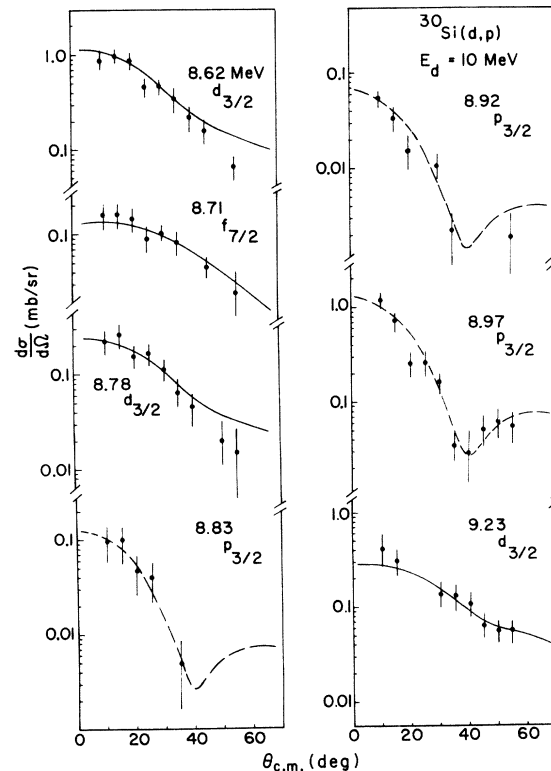


FIG. 5. Experimental angular distributions and results of DWBA calculations for states of ^{31}Si from 8.62 to 9.23 MeV in excitation. The solid curves are DWBA predictions, and extracted spectroscopic factors are summarized in Table I. The dashed curves for $p_{3/2}$ assignments are shape fits only. See Sec. IV B of the text.

factors were obtained using the usual separation-energy prescription. The geometry of the real potential for both bound and unbound states was such that $r_0 = r_{s_0} = 1.18$ fm, $a = a_{s_0} = 0.73$ fm, and $V_{s_0} = 6$ MeV. The depth of the real volume Woods-Saxon potential was adjusted for each state to fit the experimental separation energy or resonance energy. The single-particle widths calculated for the unbound states in the course of the analysis are also given in Table I. To obtain the neutron width of the resonance, in terms of the single-particle width Γ_n^{sp} and the spectroscopic factor C^2S , one has simply $\Gamma_n = C^2S\Gamma_n^{sp}$. In Fig. 6, to be discussed later, we see the neutron width Γ_n for the d and f states observed between 6 and 9 MeV in excitation, plotted as a function of excitation.

The optical potentials used in all the DWBA calculations are just those of Wildenthal and Glaudemans.³ Earlier work by the present authors¹¹ has shown that these potentials give a very good fit to the angular distributions of lower-lying states. The spectroscopic factors resulting from our DWBA analyses for bound and unbound states are summarized in Table I.

A number of interesting questions have been raised concerning ^{31}Si as a result of earlier experimental^{3,4} and theoretical¹² work. Large-basis shell model calculations of Wildenthal *et al.*¹² assumed active $d_{5/2}$, $s_{1/2}$, and $d_{3/2}$ single-particle states, with no more than two allowed vacancies in the $d_{5/2}$ state. These calculations have had reasonable success in accounting for the states in ^{31}Si below 5 MeV in excitation; compare Fig. 4. of Ref. 12 with Fig. 31.1 of Ref. 13. Predicted

spectroscopic factors are in reasonable agreement with experiment.¹² Above 5 MeV in excitation, the systematics of the shell model suggest that the single-neutron spectrum will be dominated by $d_{3/2}$, $f_{7/2}$, and $p_{3/2}$ states. This expectation is largely borne out by the present data and analysis, as we will show.

We now discuss the situation with regard to each particular orbital angular momentum transfer. In general, it should be appreciated that none of the states we observed has a spectroscopic factor greater than 0.07, so that only in overwhelming numbers can any particular l assignment affect single-particle sum rules established for lower-lying states.³

A. s -states

Only three $s_{1/2}$ states are known in ^{31}Si . These are the first excited state at 0.75 MeV, the state at 4.72 MeV, and the state at 5.27 MeV, whose previous $l=0$ assignment is confirmed in the present work (see Fig. 2). Four $s_{1/2}$ states are predicted by the calculations of Wildenthal *et al.*¹² so that one remains unaccounted for. However, this last $s_{1/2}$ state is predicted to have a very small spectroscopic factor. Indeed the spectroscopic factor for the 5.27-MeV state is already 0.04. We would have observed a fourth state if its spectroscopic factor were greater than 0.001. It therefore is unlikely that this state will be found with stripping reactions.

B. p -states

Two $p_{3/2}$ states have been observed in ^{31}Si at excitations of 3.53 and 4.38 MeV, by earlier workers.^{3,13} In our experiment, we found four possible p states, at 5.87, 8.83, 8.92, and 8.97 MeV (see Figs. 2 and 5). These states are of course not predicted in the s - d basis shell model calculations of Ref. 12. The cluster of three p states at about 9 MeV is rather interesting, and presented a problem in our DWBA analysis. These unbound states have resonance energies of more than 2 MeV and very large single-particle widths, several MeV or more. The treatment of direct reactions to unbound states upon which we rely depends upon the assumption that the single-particle width of the resonance is small compared to the energy range over which the distorted waves which make the major contribution to the (d,p) cross section vary significantly.^{1,9} Hence, although we were able to make reliable predictions of the shapes expected for $l=1$ transitions at any excitation energy, we did not attempt to predict absolute cross sections for any p -wave resonance above about 0.6 MeV resonance energy,

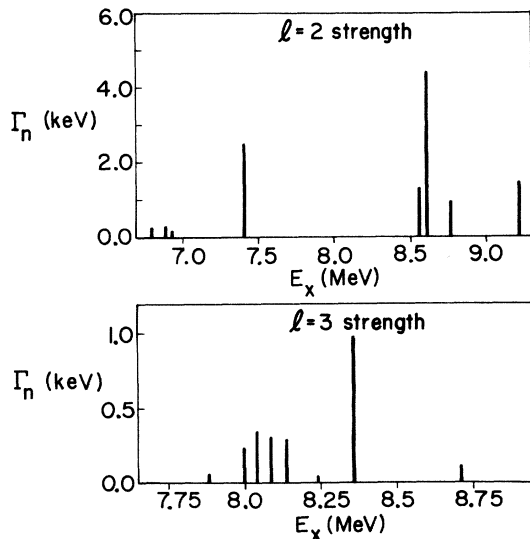


FIG. 6. Neutron widths in keV of states with orbital angular momenta 2 or 3 observed in this experiment. See Secs. IV C and IV D of the text.

corresponding to about 7.2 MeV in excitation in ^{31}Si . Thus, in Fig. 5, the angular distributions calculated for the three highest p -wave resonance states are shape fits only, and are therefore dashed in rather than being drawn as solid lines. The shape is rather distinctive, and there is little reason to doubt the $l=1$ assignment.

It is interesting that in the work of Medsker *et al.*,⁷ which was published after the present analysis was completed and which is a study very similar to our own, of $^{28}\text{Si}(d,p)$ to levels in ^{29}Si at excitations of 7.6 to 10.5 MeV, the first unbound p state is also found to be located at an excitation of around 9 MeV. The clustering of the $l=1$ strength is remarkably similar to what we observe in the present study. Indeed, the absence of p states between 5.8 and 8.8 MeV in ^{31}Si is quite striking, considering the good angular momentum match for $l=1$ at these energies. In the study of ^{29}Si , Medsker *et al.* had available recent results of $^{28}\text{Si}(n,\gamma)$ and total neutron cross section studies, which permitted independent confirmation of their mapping of p -wave strength. No such data are available for ^{31}Si ¹³ but the similarity of the two (d,p) analyses is significant.

C. d -states

The calculations of Wildenthal *et al.*, predict for the range of excitation between 0 and 5 MeV in ^{31}Si equal numbers of $d_{5/2}$ and $d_{3/2}$ states. Apart from the ^{31}Si ground state, all the predicted $d_{3/2}$ states have spectroscopic factors of 0.05 or less, as do all the predicted $d_{5/2}$ states. These expectations are largely confirmed by experiment.^{3,12} In the present data, we cannot of course distinguish between $d_{5/2}$ and $d_{3/2}$ transitions, since the familiar (d,p) j dependence disappears at excitations of 4 MeV or more. However, we have observed a rather beautiful j dependence for the angular distributions of lower-lying $l=2$ states, which cannot be accounted for by the usual DWBA description of

(d,p) reactions. We have shown elsewhere that this j dependence is very well explained by coupled-channel Born approximation (CCBA) calculations taking into account inelastic contributions to the reaction, occurring mainly in the exit proton channels.¹¹

Our data are dominated by $l=2$ and 3 transitions. Of the states we could analyze between 5.3 and 9.4 MeV, 10 are assigned $l=2$ with fair certainty, as shown in Table I and Figs. 2-5. According to the calculations of Wildenthal *et al.*, the spectroscopic strength for $d_{5/2}$ is essentially gone for excitations above 4 MeV, while perhaps 20% remains for $d_{3/2}$. Thus, in Table I we have arbitrarily assumed that all $l=2$ transitions are $d_{3/2}$. It cannot, of course, be ruled out that a few of these transitions are in fact $d_{5/2}$, since the spectroscopic factors range from 0.07 to 0.001.

The sum rule strength for $d_{3/2}$, with this assumption and the use of the earlier analysis of Ref. 3, becomes 1.19 ± 0.05 , with the region of excitation above 5 MeV contributing only about 0.27 ± 0.01 to this figure. This strength is rather uniformly spread over the region of excitation covered, as shown in Fig. 6.

D. f -states

One $f_{7/2}$ state has been previously observed in ^{31}Si at an excitation of 3.13 MeV.^{3,13} In the present study, we observe eight states which can fairly reliably be assigned as $l=3$. These states, like the p states, are seemingly clustered fairly closely, in this case near an excitation of 8 MeV. The largest cross section observed, however, is for the state at 6.10 MeV, with a spectroscopic factor of 0.036. Summing the spectroscopic factors of the cluster of f states near 8 MeV yields an additional 0.05 ± 0.01 . The total sum-rule strength for $f_{7/2}$ is thus brought to around 0.66 ± 0.01 , again using the 10 MeV results of Ref. 3 for the lower-lying state.

[†]Research supported in part by the U. S. Atomic Energy Commission and by the Research Corporation.

¹W. R. Coker, Phys. Rev. C **7**, 2426 (1973).

²C. Newson *et al.*, Bull. Am. Phys. Soc. **19**, 521 (1974).

³B. H. Wildenthal and P. W. M. Glaudemans, Nucl. Phys. **A108**, 49 (1968).

⁴M. Betigeri, R. Bock, H. H. Duhm, S. Martin, and R. Stock, Z. Naturforsch. **21a**, 980 (1966).

⁵G. W. Hoffmann, J. McIntyre, M. Mahlab, and W. R. Coker, Nucl. Instrum. (to be published).

⁶S. Hinds and R. Middleton, quoted in Ref. 13.

⁷L. R. Medsker, H. E. Jackson, and J. L. Yntema, Phys. Rev. C **9**, 1851 (1974).

⁸W. R. Coker, Phys. Rev. C **9**, 784 (1974).

⁹W. R. Coker and G. W. Hoffmann, Z. Phys. **263**, 179 (1973).

¹⁰T. Tamura, F. J. Rybicki, and W. R. Coker, Comput. Phys. Commun. **2**, 94 (1971).

¹¹G. W. Hoffmann, T. Udagawa, W. R. Coker, J. McIntyre, and M. Mahlab, Phys. Lett. **50B**, 249 (1974).

¹²B. H. Wildenthal, J. B. McGrory, E. C. Halbert, and H. D. Graber, Phys. Rev. C **4**, 1708 (1971).

¹³P. M. Endt and C. Van der Leun, Nucl. Phys. **A214**, 1 (1972).